

Sneutrino Dark Matter in Gauged Inverse Seesaw Models for Neutrinos

Haipeng An^{1,2}, P. S. Bhupal Dev¹, Yi Cai³, and R. N. Mohapatra¹

¹*Maryland Center for Fundamental Physics and Department of Physics,
University of Maryland, College Park, MD 20742, USA*

²*Perimeter Institute, Waterloo, Ontario N2L 2Y5, Canada and*

³*Department of Physics, Shanghai Jiao Tong University, Shanghai 200240, China*

Extending the Minimal Supersymmetric Standard Model (MSSM) to explain small neutrino masses via the inverse seesaw mechanism can lead to a new light supersymmetric scalar partner which can play the role of inelastic dark matter (iDM). It is a linear combination of the superpartners of the neutral fermions in the theory (the light left-handed neutrino and two heavy Standard Model singlet neutrinos) which can be very light with mass in $\sim 5 - 20$ GeV range, as suggested by some current direct detection experiments. The iDM in this class of models has keV-scale mass splitting, which is intimately connected to the small Majorana masses of neutrinos. We predict the differential scattering rate and annual modulation of the iDM signal which can be testable at future Germanium- and Xenon-based detectors.

Introduction – A plethora of cosmological observations have clearly established the existence of a dark matter (DM) component to the matter budget of the Universe, which is about five times that of the visible matter contribution. The mass and interaction properties of the DM are however not known, and experimental efforts are under way to detect it via its scattering against different kinds of nuclei, which will not only provide additional direct evidence for its existence, but will also reveal the detailed nature of its interaction with matter. Since no particle in the Standard Model (SM) can play the role of DM, this will also be a sensitive probe of physics beyond SM and supplement the new physics search at Large Hadron Collider (LHC). Supersymmetric extensions of SM provide one class of such models with several natural candidates for DM (e.g. neutralino, gravitino, etc) when R -parity symmetry is assumed. However, if the DM mass turns out to be in the few GeV range, as suggested by some recent experiments [1], the minimal version (MSSM) may need to be extended to accommodate this, mainly due to its inability to reproduce the observed DM relic density [2].

Another reason for considering extensions of MSSM is to explain small neutrino masses. It would be interesting to see if the same extensions can also provide a new DM candidate and determine its properties. Simple ways to understand the smallness of neutrino masses are by adding one or more heavy SM singlet fermions to the MSSM. In these cases, the superpartner(s) of the singlet neutrino(s) with a small admixture of the left sneutrino can play the role of DM. In this paper, we focus on the supersymmetric inverse seesaw models [3] where one adds two SM singlet fermions N and S . In these models, there are three lepton number carrying electrically neutral fermions per family, namely (ν, N, S) . The DM particle is the lightest super-partner (LSP) of the

model which can be a linear combination of the superpartners of (ν, N, S) [4–7]. Current literature on the subject discusses two classes of such models. In the first class, inverse seesaw is considered within the framework of MSSM [4]; however, in these models, one needs to omit terms in the superpotential that are allowed by the symmetries of the Lagrangian. The second class of inverse seesaw DM models extend the gauge symmetry to $SU(2)_L \times U(1)_Y \times U(1)_{B-L}$ so that the inverse seesaw mass matrix arises from a $B - L$ gauge symmetry [5]. However, the $B - L$ gauge symmetry discussed in Ref. [5] does not arise from a grand unified theory (GUT). Yet, a third class uses global $B - L$ symmetry to restrict the inverse seesaw matrix to the desired form [6]. In this letter, we extend the MSSM gauge group to the supersymmetric Left-Right (SUSYLR) gauge group $SU(2)_L \times SU(2)_R \times U(1)_{B-L}$ so that not only does the inverse seesaw matrix arise naturally but, as was shown in Ref. [8], this model can emerge as a TeV scale theory from $SO(10)$ GUT implying different dynamical properties of the DM particle than the previous works.

Working within this new class of models, we find the following results: (i) A linear combination of the superpartners of the new SM singlet fermions can be the LSP with mass from a few GeV up to about 100 GeV without running into conflict with known low energy observations. (ii) The S -fermion, which is given a small lepton number violating mass to understand small neutrino masses, leads to a splitting of the above complex scalar LSP into two closely-spaced real scalar fields, the lighter of which (we'll denote it by χ_1) is the true DM field and is accompanied by its slightly heavier partner field (χ_2) with a mass difference of order keVs. A consequence of this is that the direct detection process involves a dominantly inelastic scattering mode with the nucleus (\mathcal{N}) where $\chi_1 + \mathcal{N}(\mathcal{A}, \mathcal{Z}) \rightarrow \chi_2 + \mathcal{N}(\mathcal{A}, \mathcal{Z})$ [9], and can therefore be

tested in direct DM detection experiments [10]. The inelastic property arises naturally since the gauge Noether current coupling to the Z (and Z' in models with extended gauge symmetries) necessarily connects χ_1 to χ_2 ; also, any possible elastic contribution (mostly through the Higgs mediation) is highly suppressed due to small Yukawa couplings to light quarks. We believe this is an important point which has not been properly emphasized in earlier papers. (iii) The new TeV scale gauge dynamics in these models leads to new annihilation mechanisms for DM in the early Universe responsible for its current relic density.

General Structure of Supersymmetric Inverse seesaw – The inverse seesaw model [3] for neutrino masses uses the following mass matrix involving the (ν, N, S) fields:

$$\mathcal{M}_{\text{inv}} = \begin{pmatrix} 0 & M_D^T & 0 \\ M_D & 0 & M_R \\ 0 & M_R^T & \mu_S/2 \end{pmatrix}, \quad (1)$$

where we have suppressed the family index. This leads to the neutrino mass formula $M_\nu = M_D M_R^{-1} \mu_S (M_D M_R^{-1})^T$. Here the smallness of the neutrino masses arises from the small parameter μ_S , which for $M_R \sim \text{TeV}$ and $m_D \sim \text{GeV}$, has a value in the keV range.

Neglecting the keV-scale lepton number violation effect, the mass eigenstates are complex scalars in the basis of $(\tilde{\nu}, \tilde{N}^\dagger, \tilde{S})$, and the lightest sneutrino eigenstate can be written as

$$\tilde{\chi}_1 = \sum_{i=1}^3 (U^\dagger)_{1\nu_i} \tilde{\nu}_i + (U^\dagger)_{1N_i} \tilde{N}_i^\dagger + (U^\dagger)_{1S_i} \tilde{S}_i \quad (2)$$

where U is a 9×9 unitary matrix that diagonalizes the full neutrino mass matrix given by Eq. (1). We note here that since the entries in the \tilde{N}, \tilde{S} sector of the sneutrino mass matrix are $\sim \text{TeV}$, to get an LSP in the GeV-range, we do need some fine tuning; however, as shown in the next section, we are able to get the right relic abundance even with such low-mass DM. Also, from universality arguments, the model requires the sneutrino LSP to be always below $\sim 100 \text{ GeV}$, beyond which the lightest neutralino becomes the LSP.

When lepton number violation is invoked, the splitting terms $\sum_{m,n=1}^9 A_{mn} \tilde{\chi}_m \tilde{\chi}_n$ can be generated in the sneutrino sector (similar to those in Ref. [11]), and up to leading order in the lepton number violating mass term μ_S , the mass splitting of LSP can be written as

$$\delta M_\chi = 4|A_{11}|/M_\chi, \quad (3)$$

where generically $A_{11} \sim \mu_S M_{\text{SUSY}}$. If M_χ is also of order of the SUSY breaking scale (assumed to be around TeV), the splitting is of order μ_S , and if M_χ is much lower than

M_{SUSY} as in some region of parameter space in SUSYLR, the splitting can be enhanced.

The mass matrix in Eq. (1) arises in the SUSYLR model [8], after symmetry breaking, from the superpotential

$$\mathcal{W} = \mathcal{W}_{\text{MSSM}} + Y_\nu L \Phi L^c + Y_S S \phi_R L^c + \frac{1}{2} S \mu_S S, \quad (4)$$

where Φ is a bi-doublet under $SU(2)_L \times SU(2)_R$ with $B - L$ charge zero, and ϕ_R is a right-handed doublet with a $B - L = 1$ responsible for $B - L$ breaking.

Relic Density – From Eq. (2), we see that the sneutrino DM is a linear combination of the $(\tilde{\nu}, \tilde{N}^\dagger, \tilde{S})$ fields. Therefore, as shown in Fig. 1, its annihilation channels involve three major contributions, one from each component. Note that the second and third channels are the new contributions in SUSYLR. To leading order, the expressions for the annihilation cross sections in the s - and t -channel are respectively given by

$$\begin{aligned} \sigma_s &\simeq \frac{g_{2L}^4 \kappa_f N_c}{96\pi \cos^4 \theta_W} \frac{sv}{(s - M_Z^2)^2 + M_Z^2 \Gamma_Z^2} \left[c_0^2 + c_1^2 \left(\frac{g_{2R}}{g_{2L}} \right)^4 \right. \\ &\quad \times \left(\frac{\cos^{12} \theta_W}{\cos^2 2\theta_W} \right) \left(\frac{(s - M_Z^2)^2 + M_Z^2 \Gamma_Z^2}{(s - M_{Z'}^2)^2 + M_{Z'}^2 \Gamma_{Z'}^2} \right) \\ &\quad + 2c_0 c_1 \left(\frac{g_{2R}}{g_{2L}} \right)^2 \frac{\cos^8 \theta_W}{\cos 2\theta_W} \\ &\quad \left. \times \left(\frac{(s - M_Z^2)(s - M_{Z'}^2) + M_Z M_{Z'} \Gamma_Z \Gamma_{Z'}}{(s - M_{Z'}^2)^2 + M_{Z'}^2 \Gamma_{Z'}^2} \right) \right] \\ \sigma_t &\simeq \frac{Y_S^4 c_2^2}{96\pi} \frac{sv}{\left(M_{\phi_R}^2 - M_\chi^2 \right)^2} \end{aligned} \quad (5)$$

where $\kappa_f = (I_{3f} - Q_f \sin^2 \theta_W)^2 + (Q_f \sin^2 \theta_W)^2$, $N_c = 3(1)$ for quarks (leptons), $v = \sqrt{1 - 4M_\chi^2/s}$ is the speed of the DM particle in the center-of-mass frame, and $c_{(0,1,2)} = \sum_{i=1}^3 |U_{(\nu, N, S) i1}|^2$. We note that both s - and t -channel annihilations in our case are p -wave scattering, as expected from symmetry arguments. For low-mass DM ($M_\chi < 20 \text{ GeV}$), and assuming $Y_S \sim \mathcal{O}(1)$ and $M_{\phi_R} \lesssim 500 \text{ GeV}$, the t -channel involving only leptonic final states turns out to be the dominant contribution in our case. For this reason, we do not show the interference term between s - and t -channels for leptonic final states in Eq. (5).

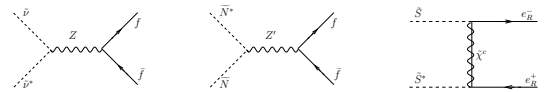


FIG. 1. The dominant annihilation channels of the sneutrino DM in SUSYLR model.

The annihilation cross section for the Z' -channel is suppressed compared to the Z -channel by a factor $(c_1/c_0)^2 (M_Z/M_{Z'})^4$. Also, we find that the correct DM relic

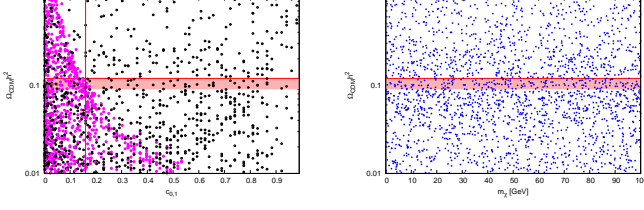


FIG. 2. In the left-panel, the purple (black) points correspond to the allowed values in the $c_{0(1)}$ -relic density plane, for the mixed sneutrino DM in our model; the vertical line shows the upper limit for c_0 from invisible Z -width constraint. The right-panel shows the scatter plot of the predictions for the LSP relic density; we find enough parameter range where the correct relic density is reproduced for a light DM. The horizontal shaded region is the 3σ limit obtained from 7-year WMAP data.

density is obtained only for $c_0 < 0.16$, as shown in the left-panel of Fig. 2. This also agrees with the invisible Z -decay width constraint (as shown by the vertical line in Fig. 2). The right panel of Fig.2 shows the scatter plot of the predictions for the LSP relic density; we find enough parameter range where the correct relic density is reproduced for a light DM.

Direct Detection – As the sneutrino DM ($\tilde{\chi}_1$) in inverse seesaw is a real scalar field accompanied by its slightly heavier partner field, it has both elastic and inelastic interaction with nuclei in direct detection experiments.

The direct detection channel mediated by the SM-like Higgs boson is due to the interaction term $\lambda h_0 \tilde{\chi}_1^\dagger \tilde{\chi}_1$, where λ is mainly the D -term contribution which can be simplified to $(g_{2L}^2 c_0 + g_{2R}^2 c_1) v_{wk}/4$ for SUSYLR assuming the decoupling limit of the MSSM Higgs mixing angles, i.e. large $\tan\beta$ and $\alpha \simeq \beta - \pi/2$ [12]. After invoking the lepton number violation effect, a mass splitting is generated between χ_1 and χ_2 , and the interaction term can be rewritten as $\frac{\lambda}{2} h_0 (\chi_1^2 + \chi_2^2)$ which is clearly an elastic interaction.

The direct detection channel conducted by gauge bosons can be written as

$$\frac{i}{2 \cos \theta_W} \left(c_0 g_{2L} Z^\mu + c_1 \frac{\cos^2 \theta_W}{\sqrt{\cos 2\theta_W}} g_{2R} Z'^\mu \right) \times (\tilde{\chi}_1 \partial_\mu \tilde{\chi}_1^\dagger - \tilde{\chi}_1^\dagger \partial_\mu \tilde{\chi}_1), \quad (6)$$

where θ_W is the Weinberg angle. After the lepton number violation term is included, the interaction term is of the form $i Z^\mu (\chi_1 \partial_\mu \chi_2 - \chi_2 \partial_\mu \chi_1)$. Therefore, the collisions between χ_1 and nucleus conducted by gauge bosons is inelastic.

The differential scattering rate of DM particle on target nucleus in direct detection experiment can be written as

$$\frac{dR}{dE_r} = \frac{\rho_{\chi_1}}{M_\chi} \int_{|\mathbf{v}| > v_{\min}} d^3 \mathbf{v} \frac{A_{\text{eff}}^2 \bar{\sigma}_N}{2 \mu_{\chi N} |\mathbf{v}|} F^2(|\mathbf{q}|) f(\mathbf{v}), \quad (7)$$

where E_r is the nuclear recoil energy, ρ_{χ_1} is the local mass density of DM, M_χ is the mass of the DM particle, σ_N is the DM-nucleon cross section, and $\mu_{\chi N}$ is the reduced mass of DM and the target nucleus. $\bar{\sigma}$ and A_{eff} are defined as $\bar{\sigma} = (\sigma_p + \sigma_n)/2$ and $A_{\text{eff}} = \sum_{i \in \text{isotopes}} 2r_i [Z \cos \theta_N + (A_i - Z) \sin \theta_N]^2$, where r_i are relative abundances of isotopes, and

$\tan \theta_N = \mathcal{M}_n / \mathcal{M}_p$, $\mathcal{M}_{n,p}$ being the DM scattering amplitudes off neutron and proton respectively [13]. $F(|\mathbf{q}|)$ is the nuclear form factor and $f(\mathbf{v})$ is the velocity distribution of the local galaxy. v_{\min} is the minimal velocity needed to generate the nuclear recoil energy E_r , which can be written as [9]

$$v_{\min} = \frac{1}{\sqrt{2 M_N E_r}} \left(\frac{M_N E_r}{\mu_{\chi N}} + \delta \right) \quad (8)$$

where δ is the mass gap, and $\delta = 0$ corresponds to the case of elastic scattering.

In the case of elastic scattering conducted by Higgs, σ_N in Eq. (7) is the total scattering cross section which can be written as

$$\sigma_N^{\text{el}} = \frac{\lambda^2 (M_N^2 \sum_q \langle N | m_q \bar{q} q | N \rangle)^2}{4 \pi v_{wk}^2 M_h^4 (M_N + M_\chi)^2}, \quad (9)$$

whereas in the case of inelastic scattering, σ_N can be written as

$$\sigma_{p,n}^{\text{in}} = \frac{g_{2L}^4 \kappa_{p,n}}{4 \pi \cos^4 \theta_W M_Z^4} \frac{M_{p,n}^2 M_{\chi_1}^2}{(M_{\chi_1} + M_{p,n})^2} \left[c_0^2 + c_1^2 \left(\frac{g_{2R}}{g_{2L}} \right)^4 \times \left(\frac{M_Z}{M_{Z'}} \right)^4 \frac{\cos^{12} \theta_W}{\cos^2 2\theta_W} + 2 c_0 c_1 \left(\frac{g_{2R}}{g_{2L}} \right)^2 \left(\frac{M_Z}{M_{Z'}} \right)^2 \frac{\cos^8 \theta_W}{\cos 2\theta_W} \right], \quad (10)$$

where the first term in the bracket is induced by Z boson whereas the second term is due to the Z' boson in SUSYLR and the last term is due to the interference between the two. The factors $\kappa_p = \left(\frac{3}{4} - \sin^2 \theta_W \right)^2$ and $\kappa_n = \left(\frac{3}{4} \right)^2$ are due to the different coupling of the vector bosons to proton and neutron respectively.

It is important to note here that for large fractions of the left sneutrino component ($c_0 \gtrsim 10^{-3}$), the scattering is mostly dominated by the Z -exchange, and is hence inelastic. The Z' contribution to the inelastic channel is always suppressed by its mass, and similarly, the elastic cross section is 4-5 orders of magnitude smaller than the Z -dominated inelastic contribution because the coupling of the Higgs to nucleon is suppressed by light quark masses. However, for $c_0 \lesssim 10^{-4}$ and large c_1 , the inelastic contribution, suppressed by the Z' -mass, could become comparable to the elastic counterpart. This is shown in Fig. 3, where we have plotted the cross section as a function of the DM mass for various values of c_0 and c_1 . One can see that for small c_0 and large c_1 values (blue and orange curves), the cross section is dominated by the elastic channel (thin lines) for low mass DM and by inelastic channel mediated by Z' for $M_\chi \gtrsim 10$ GeV (thick lines), whereas for small or zero c_1 component (pink and green curves), the scattering is always dominated by the inelastic channel mediated by Z . It is interesting to note here that the current XENON100 data constrains most of the parameter space of the model and for large c_0 , puts an upper bound on the DM mass. This can be seen clearly from Fig. 3 where we have shown the XENON100 limits on scattering cross section for various values of the mass gap, starting from zero on the left (red solid curve, corresponding to the elastic case) to $\delta = 30, 60, 90$ and 120 keV cases. We note that for small mass gaps of order

a few keV (as expected in this model), the XENON100 constraints leave only the low mass iDM (below 20 GeV) open in this model. Similar constraints on the iDM mass can be obtained using the existing data from other direct detection experiments [16], but the XENON100 constraints are found to be the most stringent.

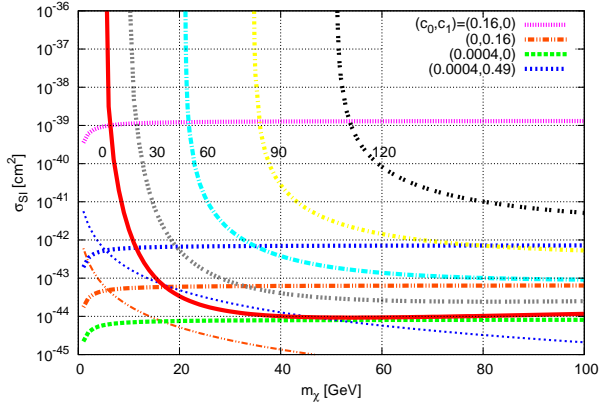


FIG. 3. The model prediction for the scattering cross section of the sneutrino DM off a nucleon as a function of its mass, for various choices of the left and right sneutrino components. Also shown are the XENON100 constraints for mass gap $\delta = (0, 30, 60, 90, 120)$ keV which were obtained by Feldman-Cousins method [14] using the 100 days of live data [15].

The nuclear recoil energy in both elastic and inelastic scattering has a maximum determined by the escape velocity of DM in the local galaxy, and a minimum determined by the mass gap for inelastic case. Therefore, the topology of the differential scattering rate for inelastic scattering is very different from the elastic scattering, which can be used to determine whether the DM is inelastic or not. Furthermore, for inelastic scattering, if the mass gap is comparable to the kinetic energy of DM, for certain nuclear recoil energy, due to Eq. (8), the required velocity is pushed to the tail end of the velocity distribution where the motion of the earth has a larger effect and therefore the DM annual modulation signal gets enhanced.

The predicted normalized differential scattering rate and annual modulation for Germanium- and Xenon-based detectors are shown in Fig. 4 with different choices for parameters of the SUSYLR model. The mass of Z' is taken to be 1 TeV in both cases. The red and blue curves are for $(c_0, c_1) = (0.001, 0.1)$ and $(c_0, c_1) = (0.1, 0.001)$, corresponding to the Z' and Z dominance, respectively, in the inelastic scattering between DM and target nucleus. The latter case is similar to the MSSM version of inverse seesaw. To translate the differential rates to experimental quantities, namely the electron equivalent recoil energies in germanium detector and the S_1 signal in xenon detector, we have used the quenching factor and scintillation efficiencies from CoGeNT [17] and XENON100 [15] experiments respectively. One can see from the first two plots in Fig. 4 that a peak shows up if the scattering is dominated by inelastic interactions. Furthermore, one can see from the third and fourth plots that for inelastic case, the annual modulation can be larger than 100% in some

energy region. Also from the solid blue curves in the first and third plots, one can see that the energy regions for large recoil energy and large modulation can be separated from each other, which provides a chance to fit the anomaly observed by the CoGeNT experiment. In these plots, A_0 and A_1 are the zeroth and first Fourier modes of the differential scattering rate; for a detailed definition, see Ref. [18].

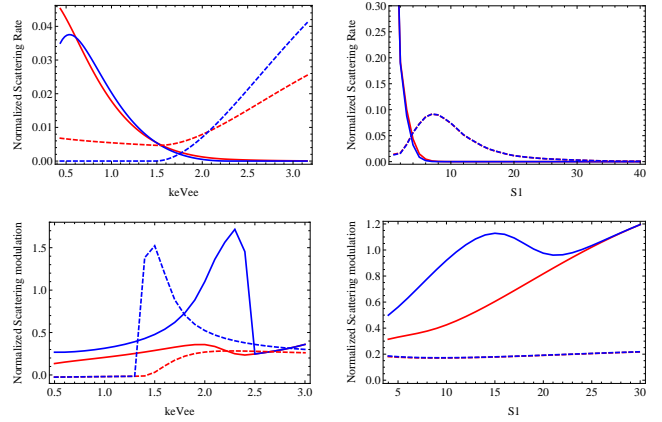


FIG. 4. The model prediction for differential scattering rates (normalized to one) and annual modulations for germanium and xenon detectors. The upper two plots show the normalized scattering rate for germanium (left) and xenon (right) detectors. The lower two plots show the annual modulation in the same detectors. Red and blue curves are for $(c_0, c_1) = (0.001, 0.1)$ and $(c_0, c_1) = (0.1, 0.001)$, respectively, while the solid and dashed curves are for $(M_\chi, \delta) = (10\text{GeV}, 20\text{keV})$ and $(50\text{GeV}, 60\text{keV})$, respectively.

We note here that it is also possible to explain the recent CRESST-II data for an iDM with mass splitting $\mathcal{O}(100)$ keV, consistent with the null results from XENON100 [19]. However, it is difficult to do so for DAMA/LIBRA, even though there still exists a narrow iDM parameter space that does fit DAMA/LIBRA data with CRESST-II [20]. For this reason, we did not include the DAMA/LIBRA results in our discussion on annual modulation.

Comments – As noted earlier, there exists a domain in the parameter space for which the dominant annihilation channel of the DM is to lepton-anti-lepton final states. The relative branching fractions depend on the masses of the RH neutrinos and are somewhat model-dependent. If we take the model in Ref. [8] as a guide, we expect them to be of similar order. These dominantly-leptonic annihilation modes can, in principle, be important in understanding signals from the galactic center, radio filaments as well as WMAP haze [21]; however, we expect these effects to be suppressed in our model due to the p -wave nature of the dominant DM annihilation channels.

Furthermore, we observe that there exist upper limits on the direct DM detection cross section from monojet plus missing energy searches in colliders [22]. However, for light spin zero dark matter only weakly interacting with the nucleons, the collider limits on the spin-independent cross sections are weaker than the direct search bounds.

Also, depending on the particle spectrum prediction of

the model, the sneutrino LSP can have distinctive collider signatures. In particular, if the gluino is lighter (heavier) than the squarks, the sneutrino LSP can have interesting four (two) jet+like (opposite)-sign dilepton signals with missing energy [23]. A detailed collider simulation of these events for our model will be given elsewhere [24].

Conclusion – To summarize, we have shown that the supersymmetric inverse seesaw model for neutrinos naturally leads to an inelastic scalar DM. The differential scattering rate and annual modulation predicted in these models might be tested in future direct detection experiments. The DM particle mass is found to be strongly constrained by the current XENON bounds, and for keV-scale mass splitting for the real scalar LSP states (as required by neutrino mass constraints), we find an upper limit of around 20 GeV on the DM mass. This is consistent with the model prediction for the sneutrino LSP mass which is required to be below ~ 100 GeV from universality arguments.

Therefore, we might be able to identify SUSY inverse seesaw if from the collider search, we can confirm that the sneutrino is a long-lived particle, and from direct detection experiments, we observe an inelastic WIMP from the differential scattering rate and the annual modulation.

Acknowledgment – H. A. and Y. C. would like to thank X. G. He for helpful discussions. H. A. is supported by the U. S. Department of Energy via grant DE-FG02-93ER-40762 and the research at Perimeter Institute is supported in part by the Government of Canada through NSERC and by the Province of Ontario through MEDT. The work of B. D. and R. N. M. is supported by National Science Foundation grant number PHY-0968854. Y. C. is supported by NSC, NCTS, NNSF and SJTU Innovation Fund for Post-graduates and Postdocs.

-
- [1] R. Bernabei *et al.* [DAMA Collaboration], Eur. Phys. J. **C 56**, 333 (2008) [arXiv:0804.2741 [astro-ph]]; *ibid* Eur. Phys. J. **C 67**, 39 (2010) [arXiv:1002.1028 [astro-ph.GA]]; C. E. Aalseth *et al.* [CoGeNT Collaboration], Phys. Rev. Lett. **106**, 131301 (2011) [arXiv:1002.4703 [astro-ph.CO]]; G. Angloher *et al.* [CRESST-II Collaboration], arXiv:1109.0702 [astro-ph.CO].
 - [2] D. Hooper, T. Plehn, Phys. Lett. **B562**, 18 (2003) [hep-ph/0212226].
 - [3] R. N. Mohapatra, Phys. Rev. Lett. **56**, 561 (1986); R. N. Mohapatra and J. W. F. Valle, Phys. Rev. D **34**, 1642 (1986).
 - [4] C. Arina, F. Bazzocchi, N. Fornengo, J. C. Romao, J. W. F. Valle, Phys. Rev. Lett. **101**, 161802 (2008) [arXiv:0806.3225 [hep-ph]].
 - [5] S. Khalil, H. Okada, T. Toma, JHEP **1107**, 026 (2011) [arXiv:1102.4249 [hep-ph]].
 - [6] F.-X. Josse-Michaux, E. Molinaro, arXiv:1108.0482 [hep-ph].
 - [7] Z. Kang, J. Li, T. Li, T. Liu, J. Yang, [arXiv:1102.5644 [hep-ph]].
 - [8] P. S. Bhupal Dev, R. N. Mohapatra, Phys. Rev. D **81**, 013001 (2010) [arXiv:0910.3924 [hep-ph]]; Phys. Rev. D. **82**, 035014 (2010) [arXiv:1003.6102 [hep-ph]].
 - [9] D. Tucker-Smith, N. Weiner, Phys. Rev. **D64**, 043502 (2001).
 - [10] D. Tucker-Smith, N. Weiner, Nucl. Phys. Proc. Suppl. **124**, 197-200 (2003) [astro-ph/0208403].
 - [11] J. March-Russell, C. McCabe, M. McCullough, JHEP **1003**, 108 (2010) [arXiv:0911.4489 [hep-ph]].
 - [12] S. P. Martin, In G. L. Kane (ed.), *Perspectives on supersymmetry*, pp. 1-98 [arXiv:hep-ph/9709356 [hep-ph]].
 - [13] J. L. Feng, J. Kumar, D. Marfatia, D. Sanford, Phys. Lett. **B703**, 124-127 (2011) [arXiv:1102.4331 [hep-ph]].
 - [14] G. J. Feldman, R. D. Cousins, Phys. Rev. **D57**, 3873-3889 (1998) [physics/9711021 [physics.data-an]].
 - [15] E. Aprile *et al.* [XENON100 Collaboration], Phys. Rev. Lett. **107**, 131302 (2011) [arXiv:1104.2549 [astro-ph.CO]]; Phys. Rev. **D84**, 061101 (2011) [arXiv:1104.3121 [astro-ph.CO]].
 - [16] R. Bernabei *et al.* [DAMA Collaboration], Eur. Phys. J. **C23**, 61-64 (2002); D. Y. Akimov *et al.* [ZEPLIN-III Collaboration], Phys. Lett. **B692**, 180-183 (2010) [arXiv:1003.5626 [hep-ex]]; Z. Ahmed *et al.* [CDMS-II Collaboration], Phys. Rev. **D83**, 112002 (2011) [arXiv:1012.5078 [astro-ph.CO]].
 - [17] C. E. Aalseth *et al.* [CoGeNT Collaboration], Phys. Rev. Lett. **107**, 141301 (2011) [arXiv:1106.0650 [astro-ph.CO]].
 - [18] H. An, F. Gao, [arXiv:1108.3943 [hep-ph]].
 - [19] J. Kopp, T. Schwetz, J. Zupan, arXiv:1110.2721 [hep-ph].
 - [20] S. Chang, R. F. Lang, N. Weiner, Phys. Rev. Lett. **106**, 011301 (2011) [arXiv:1007.2688 [hep-ph]].
 - [21] M. R. Buckley, D. Hooper, J. L. Rosner, Phys. Lett. **B703**, 343 (2011) [arXiv:1106.3583 [hep-ph]]; D. Hooper, T. Linden, arXiv:1110.0006 [astro-ph.HE].
 - [22] J. Goodman, M. Ibe, A. Rajaraman, W. Shepherd, T. M. P. Tait and H. -B. Yu, Phys. Rev. D **82**, 116010 (2010) [arXiv:1008.1783 [hep-ph]]; P. J. Fox, R. Harnik, J. Kopp and Y. Tsai, arXiv:1109.4398 [hep-ph].
 - [23] G. Belanger, S. Kraml, A. Lessa, JHEP **1107**, 083 (2011) [arXiv:1105.4878 [hep-ph]].
 - [24] H. An, P. S. Bhupal Dev, Y. Cai, R. N. Mohapatra, in preparation.